Injectable, Self-Gelling, Biodegradable, and Immunomodulatory DNA Hydrogel for Antigen Delivery

Makiya Nishikawa,[1,*] Kohei Ogawa,[1] Yuka Umeki,[1] Kohta Mohri,[1] Yohji Kawasaki,[2] Hiroshi Watanabe,[2] Natsuki Takahashi,[1] Eri Kusuki,[1] Rei Takahashi,[3] Yuki Takahashi,[1] and Yoshinobu Takakura[1]

[1]Department of Biopharmaceutics and Drug Metabolism, Graduate School of Pharmaceutical Sciences, Kyoto University, Sakyo-ku, Kyoto 606-8501, Japan. [2]Institute for Chemical Research, Kyoto University, Gokasho, Uji, Kyoto 611-0011, Japan. [3]Department of Pharmacotherapeutics, Faculty of Pharmaceutical Sciences, Doshisha Women's College of Liberal Arts, Kyotanabe, Kyoto 610-0395, Japan.

Corresponding Author
Makiya Nishikawa, Ph.D., Department of Biopharmaceutics and Drug Metabolism, Graduate School of Pharmaceutical Sciences, Kyoto University, Sakyo-ku, Kyoto 606-8501, Japan. Telephone: +81-75-753-4580. E-mail: makiya@pharm.kyoto-u.ac.jp

ABSTRACT
DNA nanotechnology-based nanosystems and macrosystems have attracted much attention in the biomedical research field. The nature of DNA endows these systems with biodegradable, biocompatible, and immunomodulatory properties. Here, we present an injectable hydrogel system that consists only of chemically synthesized short DNA strands, water, and salts. Several preparations of polypod-like structured DNA, or polypodna, were designed, including tri-, tetra-, penta- and hexapodna, as the building blocks of self-gelling DNA hydrogel. Under physiological conditions, properly designed polypodna preparations formed a hydrogel. The analysis of the modulus data of the hydrogel consisting of two sets of hexapodna preparations showed that this injectable hydrogel was reorganized in a time scale of 0.25 s. Then, DNA hydrogel containing unmethylated cytosine-phosphate-guanine (CpG) dinucleotides was used to stimulate innate immunity through Toll-like receptor 9, the receptor for CpG DNA. Gel formation significantly increased the activity of immunostimulatory CpG DNA, retarded the clearance after intradermal injection into mice, and increased the immune responses to ovalbumin (OVA) incorporated into the hydrogel as a model antigen. OVA/CpG DNA hydrogel induced much less local or systemic adverse reactions than OVA injected with complete Freund's adjuvant or alum. GpC DNA hydrogel containing no CpG sequences was less effective, indicating the importance of immunomodulation by CpG DNA hydrogel. Thus, we have created an efficient system for sustained delivery of antigens or other bioactive compounds.

Keywords: hydrogel, CpG motif, controlled release, antigen, immune cell, self-gelling

INTRODUCTION

Natural, biocompatible, and biodegradable materials are optimal properties of potential drug delivery systems. DNA fits these criteria because it has been naturally selected for the storage, transmission, and expression of genetic information. Recent progress in DNA nanotechnology research has facilitated the design and construction of a variety of DNA-based nano-sized structures [1-5]. Although these designs are esthetically satisfying, most of these systems have not yet been applied to the pharmaceutical or therapeutic fields.

DNA also has immunomodulatory properties when present in the cytosol or outside cells. DNA containing unmethylated cytosine-phosphate-guanine (CpG) dinucleotides, or CpG DNA [6,7] is a potent stimulator of innate immunity, as it is the ligand for the Toll-like receptor 9 (TLR9) [8]. CpG DNA induces the production of helper T-cell type 1 cytokines, and its clinical potential is being investigated in several indications, including cancer [9-11]. Phosphorothioate (PS)-stabilized CpG DNA is the form most frequently used in clinical trials [12,13], although it is associated with renal toxicity. We propose that polypod-like structured DNA, or polypodna for short, consisting of three or more oligodeoxynucleotides (ODNs) is a novel and alternative approach to increasing the immunostimulatory activity of CpG DNA, without the requirement for PS stabilization [14,15].

Connecting multiple tetrapodna (X-DNA) units results in the formation of DNA hydrogel, as first reported by Um et al [16]. We extended these results by replacing the DNA sequences with those containing immunostimulatory CpG motifs [17]. In these studies, palindromic four nucleotides at the 5'-ends of ODNs were ligated using T4 DNA ligase to obtain DNA hydrogels. The CpG DNA hydrogel containing doxorubicin was effective in inhibiting tumor growth in mice, but the administration of the hydrogels required surgical incision, or breaking them down into fragments small enough for injection. A more important issue with pre-existing DNA hydrogel formulations is that the contaminating ligase can trigger unwanted responses, including anaphylactic shock. Therefore, the development of ligation-free and injectable DNA hydrogels would greatly improve the potency of DNA hydrogels as sustained delivery systems. There are few reports on the preparation of DNA hydrogels without the use of DNA ligase [18,19] and no injectable DNA hydrogels have been reported thus far.

Here we present a novel method to develop ligase-free, injectable DNA hydrogel. To this end, the single stranded 5'-ends of polypodna were extended to hybridize under physiological conditions. These hydrogels were easily injected using a fine gauge needle, and gelation occurs almost instantly following injection. Finally, we show that the DNA hydrogel can efficiently deliver tumor antigens with higher potency and less toxicity than clinically available vaccine adjuvants.

MATERIALS AND METHODS

Animals and cell culture. Four-week-old ICR mice and six-week-old C57BL/6 mice were purchased from Japan SLC, Inc. (Shizuoka, Japan). All animal experiments were conducted in accordance with the principles and procedures outlined in the National Institutes of Health Guide for the Care and Use of Laboratory Animals. The protocols for animal experiments were approved by the Animal Experimentation Committee of Graduate School of Pharmaceutical Sciences, Kyoto University. Mouse dendritic DC2.4 cells were a gift from Dr. K. L. Rock, University of Massachusetts Medical School, Worcester, MA, USA. CD8OVA1.3 cells, a mouse T cell hybridoma against an OVA class I epitope, were a gift from Dr. C. V. Harding, Case

Western Reserve University, Cleveland, OH, USA. EL4, a T lymphoma, and EG7-OVA, an OVA transfectant of EL4, were purchased from American Type Culture Collection (Manassas, VA, USA). Cell culture was performed as previously described [20].

Preparation of polypodna and DNA hydrogel. All phosphodiester ODNs were purchased from Integrated DNA Technologies, Inc. (Coralville, IA, USA). The sequences of the ODNs are summarized in Table S1. Polypodna preparations were prepared by mixing equimolar ODNs as previously described [15], and the formation was confirmed by 6% polyacrylamide gel electrophoresis (PAGE). DNA hydrogel was obtained by increasing the salt or DNA concentration of polypodna solution, or by mixing different units of polypodna or other forms of DNA assemblies, such as double stranded DNA (dsDNA). The hydrogel formation was briefly checked by adding solution containing blue dextran (Sigma-Aldrich, St. Louis, MO, USA), because it does not instantly diffuse into hydrogel. The inner structure of DNA hydrogel was observed using a field-emission scanning electron microscope (FE-SEM: S4700, HITACHI, Japan) as previously described [17]. The melting temperature (Tm) was obtained with a Shimadzu UV-1600 PC spectrometer (Kyoto, Japan) equipped with a TMSPC-8 temperature controller as previously described [15].

Measurement of viscoelastic properties of DNA hydrogel. Rheological behavior of DNA hydrogels was examined with a laboratory rheometer (ARES; Rheometric Scientific currently TA Instruments, USA) at room temperature (~25 °C). A parallel-plate fixture with the diameter of 8.0 mm was used for oscillatory and steady flow tests, following a standard protocol of rheological test [21].

IL-6 release from DC2.4 cells or in mice. DNA samples were added to DC2.4 cells at the indicated concentrations and the cells were incubated for 16 h. Then, the supernatant was collected and the concentration of IL-6 was determined by ELISA following the manufacturer's protocol (BD Biosciences, San Diego, CA, USA). Serum samples of mice receiving an intradermal injection of 220 μg DNA were also subjected to ELISA.

Radiolabeling of ODN. An ODN (ssDNA(GpC)$_{8np-32}$-A1) was end-labeled with ^{32}P using [γ-^{32}P]ATP and T4 polynucleotide kinase (T4 PNK; Takara Bio, Otsu, Japan) according to the manufacturer's instructions, and purified using NAP5 columns (GE Healthcare, Tokyo, Japan). ^{32}P-DNA was used to obtain ^{32}P-ssDNA(CpG), ^{32}P-hexapdna(CpG) or ^{32}P-DNA hydrogel(CpG).

Tissue distribution of radioactivity after intradermal injection of ^{32}P-DNA. ICR mice were intradermally injected with ^{32}P-DNA at a dose of 10 mg DNA/kg (220 μg DNA/mouse). At the indicated times after injection, mice were anesthetized and the injection site and draining lymph nodes were collected and processed as previously reported [22]. Then, the radioactivity in these tissue samples was counted in a Tri-Carb 3110 TR counter (Perkin–Elmer, Norwalk, CT, USA).

Quantitative measurement of IL-6 mRNA expression. Under anesthesia with isoflurane, C57BL/6 mice were injected with 220 μg DNA. At the indicated time points after injection, mice were anesthetized and the injection site and draining lymph nodes were excised. The total RNA was extracted from the skin tissues using an RNeasy mini kit (QIAGEN GmbH, Hilden, Germany) in accordance with the manufacturer's protocol. Total RNA from the draining lymph

nodes was extracted using Sepasol RNA I super (Nacalai Tesque). The extracted RNA was reverse-transcribed with a ReverTra Ace® qPCR RT Kit (TOYOBO, Osaka, Japan). For quantitative analysis of mRNA expression, real-time PCR was conducted with total RNA using KAPA SYBR FAST ABI Prism 2X qPCR Master Mix (KAPA BIOSYSTEMS, Boston, MA, USA). The ODN primers used for amplification were as follows: IL-6, forward (5'-GTTCTCTGGGAAATCGTGGA-3') and reverse (5'-TGTACTCCAGGTAGCTATGG-3'); β-actin, forward (5'-CATCCGTAAAGACCTCTA- TGC-3') and reverse (5'-ATGGAGCCACCGATCCACA-3'). Amplified products were detected online via intercalation of SYBR Green, a fluorescent dye, by using StepOnePlus Real Time PCR System (Applied Biosystems, Foster City, CA, USA). The IL-6 mRNA expression was normalized to the mRNA level of β-actin.

OVA release from DNA hydrogel. OVA (albumin from chicken egg white, Sigma-Aldrich) was labeled with fluorescein isothiocyanate (FITC; fluorescein isothiocyanate isomer 1, Sigma-Aldrich) to obtain FITC-OVA. FITC-OVA was added to both hexapodna solutions and DNA hydrogel was prepared by mixing the solutions. Then, FITC-OVA/DNA hydrogel (10 μl) was placed into the upper chamber of the Transwell (Product#3460, 0.4 μm pore size, Corning Inc., Corning, NY, USA), and 500 μl PBS was added into the bottom chamber, and incubated at 37 °C. At predetermined time points, bright field and fluorescence images of FITC-OVA/DNA hydrogel were obtained using LAS3000 system (Fujifilm, Tokyo, Japan), and the receiver solution was collected and replaced with 500 μl fresh PBS. The fluorescence intensity of the receiver solution was measured in a Wallac 1420 ARVO MX-2 Multilabel Counter (Perkin Elmer, Boston, MA, USA).

Degradation of DNA hydrogel by DNase. Hexapodna preparations (220 μg/100 μl) were incubated at 37 °C in the presence of DNase I (0.002 U/μg of DNA). At predetermined time points, a 10 μl aliquot of the sample solution was transferred to plastic tubes and mixed with 20 μl of 0.5 M EDTA solution to stop the degradation and then stored at -20 °C until use. These samples were run on a 6 % PAGE and stained with ethidium bromide. The density of DNA bands was quantitatively evaluated using the Multi Gauge software (FUJIFILM, Tokyo, Japan). DNA hydrogel (220 μg/10 μl) was prepared in plastic tubes and incubated at 37 °C after addition of solution containing DNase I (0.002 U/μg of DNA). At predetermined time points, supernatant was removed, and amount of remaining DNA was evaluated by measuring absorbance of 260 nm at 95 °C.

Antigen presentation assay. To cultured DC2.4 cells were added DNA (2 μg/ml) and OVA (2 mg/ml), then CD8OVA1.3 cells, then the mixture was incubated at 37 °C in 5% CO_2 for an additional 24 h. The concentration of IL-2 in the supernatant was determined using an ELISA kit (mouse IL-2 BD OptEIA Set, BD Biosciences).

Immunization of mice. Under anesthesia with isoflurane, the dorsal skin of C57BL/6 mice was injected with 50 μg OVA in the presence or absence of 220 μg DNA in 10 μl saline or with complete Freund's adjuvant (CFA). Mice were immunized thrice on days 0, 7, and 14. Seven days after the last immunization, mice were killed and serum and the spleen were collected.

Measurement of OVA-specific antibody. Serum samples were serially diluted to measure the OVA-specific total IgG levels by ELISA as previously described [23].

IFN-γ secretion from spleen cells. Seven days after the last immunization, spleen cells were isolated, purified and cultured in the presence of OVA (1 mg/ml) in 96-well culture plates for 4 days. The concentration of IFN-γ in supernatant was determined by ELISA (Ready-SET-Go! Mouse IFN-γ ELISA, eBioscience, San Diego, CA, USA).

Cytotoxic T lymphocyte assay. Seven days after the last immunization, spleen cells were isolated and purified as above. To prime CTLs, splenocytes were co-cultured with mitomycin C-treated EG7-OVA cells for 5 days in 5% CO2 at 37 °C. Target cells (EG7-OVA or EL4) were labeled with ^{51}Cr-sodium chromate ($Na_2{}^{51}CrO_4$, Fujifilm RI Pharma, Tokyo, Japan). Boosted splenocytes, effector cells, were serially diluted and co-incubated with the target cells for 4 h at 37 °C. Then, the percentage of specific lysis was calculated as previously reported [20].

Hematoxylin and eosin staining of skin sections. Under anesthesia with isoflurane, the dorsal skin of C57BL/6 mice was injected with 50 μg OVA with or without 220 μg DNA, CFA or 100 μg alum (aluminum potassium sulfate dodecahydrate, Nacalai Tesque, Kyoto, Japan). Seven days after the immunization, the injection site was excised, fixed in 4% paraformaldehyde, embedded in paraffin, sliced and stained with hematoxylin and eosin. Stained samples were examined under a microscope for histological evaluation.

Measurement of spleen weight. Spleen was collected from different sets of C57BL/6 mice at seven days after the third immunization with weekly intervals. Spleen weight was measured as an indicator of splenomegaly, a systemic adverse effect of immunostimulatory compounds.

Statistical analysis. Statistical analyses were performed using Statview v. 5.0 (SAS Institute Inc., Cary, NC, USA). Statistical differences were analyzed using one-way analysis of variance (ANOVA) followed by Student-Newman-Keuls test. *P* values of 0.05 were considered significant.

RESULTS

Spontaneous formation of DNA hydrogel. Several sets of ODNs were designed to obtain polypodna preparations with three- (tripodna), four- (tetrapodna), or six-pods (hexapodna) (Table S1). The formation of these preparations was confirmed by polyacrylamide gel electrophoresis (PAGE) (Figure S1). Two sets of four ODNs with 40-nucleotide (nt) length in total and 12-nt length of single stranded 5'-ends were used to obtain tetrapodna$(CpG)_{12p\text{-}28}$-A and tetrapodna$(CpG)_{12np\text{-}28}$-A, respectively, and these were visualized using propidium iodide (PI), an intercalating dye. A tetrapodna$(CpG)_{12p\text{-}28}$-A having palindromic (p) 12-mer 5'-ends (5'-acgtcatgacgt-3') was soluble in a buffer solution containing 5 mM sodium chloride (Figure 1a, far left), and gelled upon drop wise addition into a solution containing physiological salt concentration (phosphate-buffered saline; 137 mM NaCl, 2.7 mM KCl, 10 mM Na_2HPO_4 and 1.76 mM KH_2PO_4, pH, 7.4) (Figure 1a, third from left). Another tetrapodna, tetrapodna$(CpG)_{12np\text{-}28}$-A, with non-palindromic (np) 12-mer 5'-ends (5'-acgtcagcgtta-3') diffused when added into the solution (Figure 1a, far right). A typical field emission scanning

electron microscopy image of the DNA hydrogel consisting of tetrapodna$(CpG)_{12p-28}$-A clearly shows that the DNA hydrogel has an ordered structure with abundant space within the gel (Figure 1b).

Hydrogel formation by mixing two polypodna preparations. The mixing of a polypodna and other DNA components with the 5'-ends complementary to the sequence of the polypodna will lead to hydrogel formation. This mixing strategy is useful when considering the incorporation of compounds into DNA hydrogels. Three types of hexapodna preparations, hexapodna$(GpC)_{8np-32}$-A, hexapodna$(GpC)_{8np-32}$-B and hexapodna$(GpC)_{8np-32}$-C, were designed; the first two shared complementary 5'-ends (5'-tcctgacg-3' and 5'-cgtcagga-3'), whereas the 5'-ends of the third hexapodna were not complementary to either of the other oligonucleotides. Figure 1c shows two sets of PI-labeled hexapodna preparations mixed in a 29-gauge syringe. When hexapodna$(GpC)_{8np-32}$-A and hexapodna$(GpC)_{8np-32}$-B were mixed together, DNA hydrogel (DNA hydrogel(GpC)) was quickly formed (Figure 1c, right). The water content calculated from the composition of the gel was 97.8 w/v%, indicating most of the component in the gel is water. The Tm of the 8-mer 5'-ends of hexapodna$(GpC)_{8np-32}$-A and hexapodna$(GpC)_{8np-32}$-B was calculated to be 35.0°C at DNA concentration of 24.6 μg/ml, whereas the Tm of DNA hydrogel(GpC) was 55.8°C at the same concentration, suggesting that the hybridization of the 8-mer 5'-ends of hexapodna preparations consisting of DNA hydrogel is more thermally stable than the hybridization of simple 8-mer ODNs, even though the sequences are the same. The injected DNA through the 29-gauge needle almost instantly gelled (Figure 1d, right). As shown in Figure 1e, DNA hydrogels were formed in the skin tissues of mice. In contrast, the mixture of non-complementary sets of hexapodna preparations did not form hydrogels (Figure 1c left, Figure 1d left, and Figure 1f). Similar results were obtained using other polypodna preparations (data not shown).

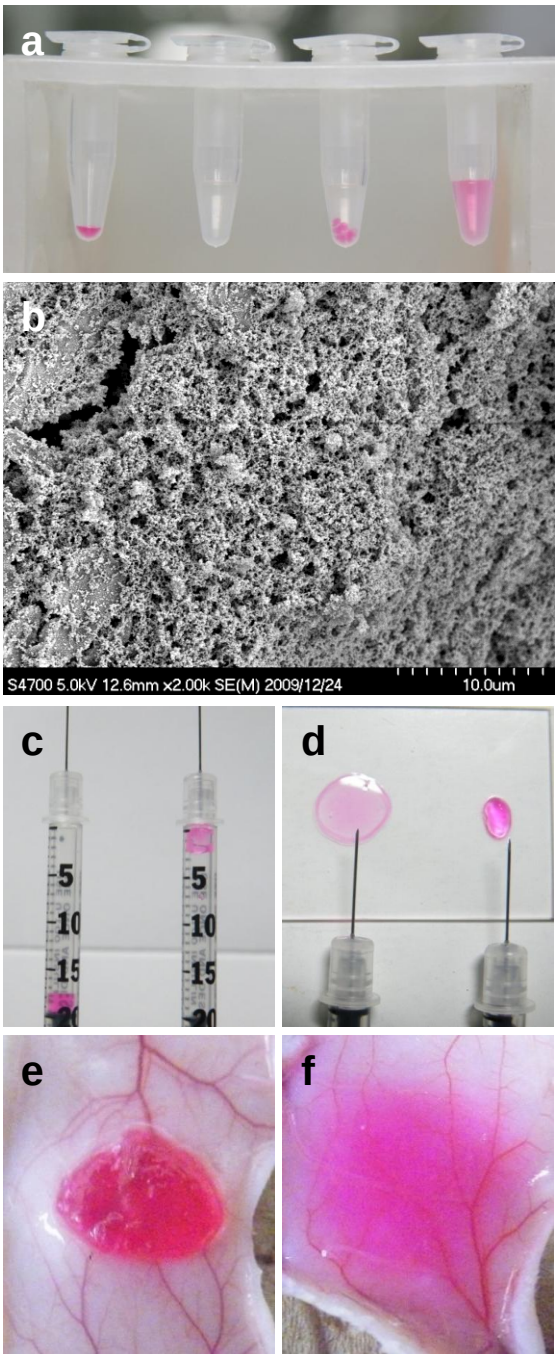

Figure 1. Formation of DNA hydrogel without DNA ligase. (a) Hydrogel formation after drop wise addition of tetrapodna preparations into a buffer solution. Tetrapodna preparations were labeled using PI. Far left, tetrapodna$(CpG)_{12p-28}$-A in a buffer solution containing 5 mM sodium chloride. Second from the left, a solution containing the physiological sodium chloride concentration of 154 mM. Third from the left,

tetrapodna$(CpG)_{12p\text{-}28}$-A added to the solution containing physiological sodium chloride concentration. Far right, tetrapodna$(CpG)_{12np\text{-}28}$-A added to the solution containing physiological sodium chloride concentration. (b) An FE-SEM image of the inner structure of DNA hydrogel consisting of tetrapodna$(CpG)_{12p\text{-}28}$-A. (c, d) Hydrogel formation in syringe and injection through a 29-gauge needle. Hexapodna$(GpC)_{8np\text{-}32}$-A and hexapodna$(GpC)_{8np\text{-}32}$-B (right, DNA hydrogel[GpC]) or hexapodna$(GpC)_{8np\text{-}32}$-A and hexapodna$(GpC)_{8np\text{-}32}$-C (left), all of which were labeled using PI, were mixed in a 29-gauge insulin syringe (c), then injected (d). (e, f) Hydrogel formation in mouse skin after intradermal injection. Hexapodna$(GpC)_{8np\text{-}32}$-A and hexapodna$(GpC)_{8np\text{-}32}$-B (e, DNA hydrogel(GpC)) or hexapodna$(GpC)_{8np\text{-}32}$-A and hexapodna$(GpC)_{8np\text{-}32}$-C (f) was injected into the dorsal skin of mice at a dose of 30 mg/kg (660 μg/mouse), and the skin was collected and observed at 3 h after injection.

Rapid recovery of the elasticity of DNA hydrogel on flow cessation. We next examined the rheological behavior of the DNA hydrogel(GpC). For each experimental run, the hydrogel was freshly prepared in a 29-gauge syringe at a total DNA concentration of 22.1 mg/ml (0.3 mM each ODN/ml) and charged in the rheometer.

Figures 2a and 2b, respectively, show the storage and loss moduli (G' and G'') of the hydrogel under oscillatory strain of various amplitudes (γ_0) as indicated. In Figure 2b, the dotted curves indicate the G' data for $\gamma_0 = 0.005$ (0.5 %) and 0.1 (10%). For $\gamma_0 \leq 0.01$ (1%), G' is independent of γ_0 and the angular frequency ω. Correspondingly, the loss modulus G" is much smaller than G', as noted from comparison of the triangles and upper dotted curve in Figure 2b. This linear elastic behavior, characterized by the equilibrium modulus $G_e = 1.1 \times 10^3$ Pa, indicates the solid-like feature of the hydrogel due to the physical network of hexapodna units not disputed under small strains.

In contrast, G' begins to decrease whereas G'' begins to increase with increasing γ_0 to 0.02 (2%). In particular, G'' becomes well above G' at the maximum strain amplitude examined, $\gamma_0 =$ 0.1 (10 %), as noted from comparison of the filled squares and lower dotted curve in Figure 2b. These features reflect nonlinear *flow* of the hydrogel under large strains. In relation to this nonlinear flow, we also note that G' for $\gamma_0 = 0.1$ exhibits a minimum at $\omega = 4$ rad/s. This minimum, rarely observed for ordinary physiological gels [24], suggests that the DNA hydrogel has a molecular process with a characteristic time τ (in s) $= 1/\omega = 0.25$. The elasticity of the hydrogel is undoubtedly sustained by the physical network of hexapodna units, and the large strain should result in reorganization (disruption followed by reformation) of the network. This reorganization appears to occur at $\tau = 0.25$ s: For ω below $1/\tau$, the network has a sufficient time to reform itself during one cycle of oscillation to exhibit larger G'. In contrast, for ω above $1/\tau$, it has an insufficient time for disruption thereby exhibiting larger G'. The minimum of G' at $\omega = 1/\tau$ possibly resulted from competition of such reformation and disruption processes. Consequently, Figure 2b shows the G''/G' ratio for $\gamma_0 = 0.1$ to become the largest at $\omega = 1/\tau$, which suggests that an efficiency thermal dissipation of the mechanical energy reflected in this ratio becomes the highest when the network is most heavily disrupted.

The corresponding nonlinearity was noted also under constant-rate shear flow. Figure 2c shows the stress $\sigma^+(t)$ of the hydrogel at a time t after start-up of the flow. The $\sigma^+(t)$ data measured for various rates κ are plotted against the strain imposed through the flow, $\gamma = \kappa t$. The dashed line denotes the linear elastic response, $\sigma^+ = G_e\gamma$ with G_e (= 1.1×10^3 Pa) being the equilibrium modulus explained earlier. The $\sigma^+(t)$ data for *all* κ values follow this line for small $\gamma < 0.03$. Thus the hydrogel behaves as an elastic solid even under flow, given that the strain does

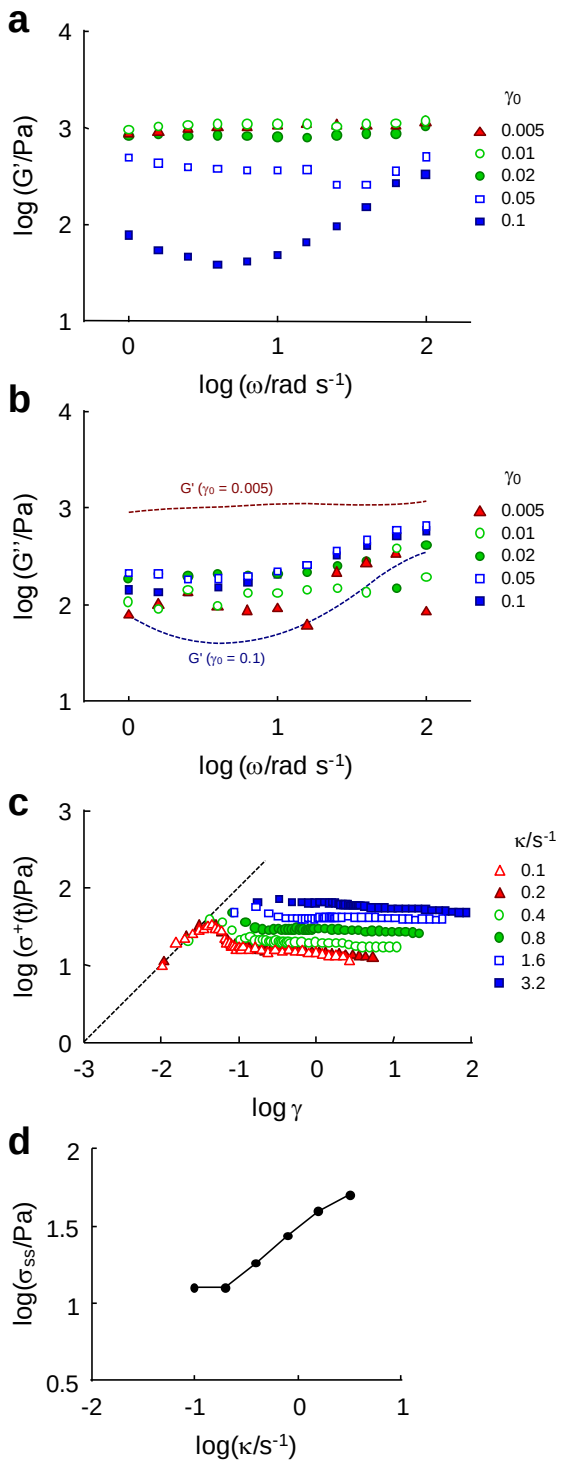

not exceed a threshold, $\gamma^* \cong 0.03$. Interestingly, this γ^* value is close to the onset of nonlinearity ($\gamma_0 \cong 0.02$) under the oscillatory strain (Figure 2a). For $\gamma > \gamma^*$ in Figure 2c, σ^+ deviates downward from the linear elastic line and decays to a steady state value σ_{ss}. This behavior reflects the "yielding" (switch from solid to fluid) under flow. In Figure 2d, those σ_{ss} values are plotted against the shear rate, κ. The σ_{ss} data approach a constant value of 13 Pa with decreasing κ, which indicates that the hydrogel has a dynamic yield stress, $\sigma_{y,dyn} \cong 13$ Pa, being necessary for reorganizing the hydrogel under steady flow. The $\sigma_{y,dyn}$ value is smaller than the static yield stress required for the network reorganization under slow strain, $\sigma_{y,dyn} \cong 32$ Pa (estimated in Figure 2c as the stress at $\gamma = \gamma^* \cong 0.03$). Thus, the network appears to be scarcer under flow than at equilibrium. Nevertheless, oscillatory tests following the steady flow showed that the equilibrium network was recovered immediately after cessation of the flow. This rapid reformation and small value of $\sigma_{y,dyn}$ enable easy injection of the DNA hydrogel into the mouse through the syringe and solidification immediately after the injection.

Figure 2. Rheological characterization of DNA hydrogel exhibiting quick reorganization of hydrogen bonds at room temperature (~25 °C). (a) and (b) Storage and loss moduli (G' and G'') measured for sinusoidal strain at various angular frequencies ω and with the amplitude γ_0 as indicated. In panels (a) and (b), respectively, the G' and G'' data are plotted against ω in the double-logarithmic scale. The dotted curves in panel (b) indicate the G' data for amplitude $\gamma_0 = 0.005$ and 0.1 (0.5% and 10 %). The minimum of G' at $\omega = 4$ s^{-1} observed for large γ_0 is indicative of the network reorganization process at a characteristic time $\tau \cong 0.25$ s. (c) Time evolution of the shear stress $\sigma^+(t)$ measured after start-up of shear flow at constant rates κ as indicated. The $\sigma^+(t)$ are plotted against the strain, $\gamma = \kappa t$. (d) Steady state shear stress σ_{ss} evaluated from the $\sigma^+(t)$ data shown in Fig. 2c. The σ_{ss} data are plotted against the shear rate κ and the dynamic yield stress, $\sigma_{y,dyn} \cong 13$ Pa, is evaluated from those data at low κ. Data shown are representative of two independent experiments.

Increased immunostimulatory activity of CpG DNA by hydrogel formation. We previously demonstrated that the immunostimulatory activity of CpG DNA is significantly increased by conversion into polypodna [14,15,17,25]. To examine the immunostimulatory activity of DNA hydrogels, several forms of DNA samples were compared in terms of interleukin-6 (IL-6) release from mouse dendritic DC2.4 cells. Figure 3a shows the amount of IL-6 released from DC2.4 cells after addition of DNA samples at the indicated concentrations. Similar to the hexapodna preparations with no single stranded 5'-ends15, hexapodna(CpG) induced a greater amount of IL-6 production than ssDNA(CpG). At equimolar concentrations, DNA hydrogel(CpG) was significantly ($P < 0.05$) more potent than hexapodna(CpG) in inducing IL-6. GpC samples induced no detectable IL-6 production, irrespective of the structures.

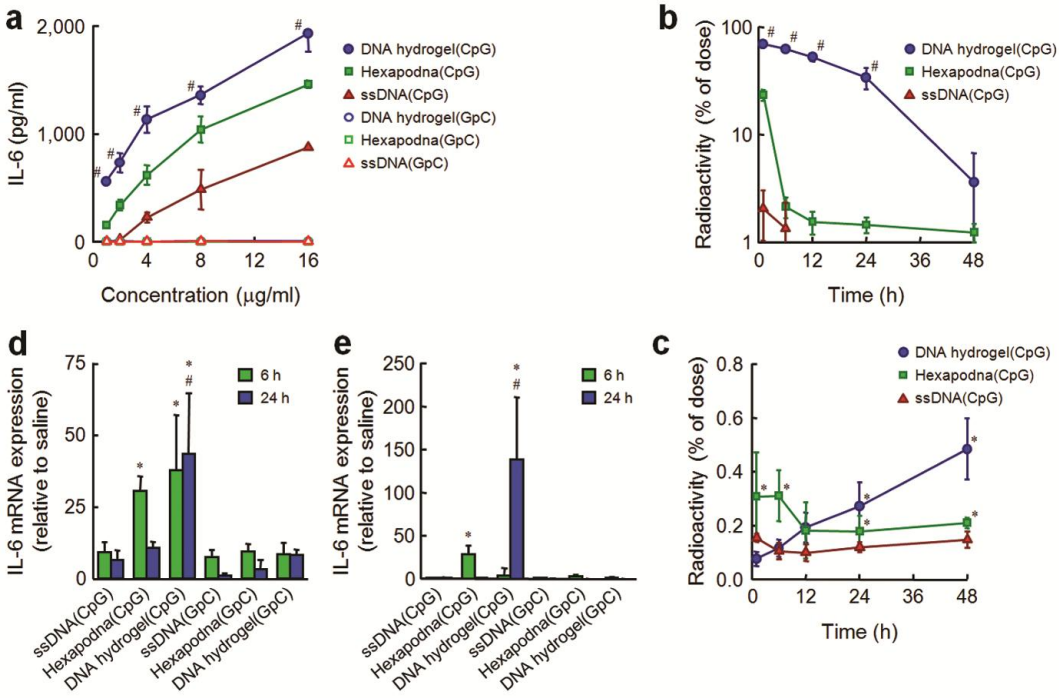

Figure 3. IL-6 production, sustained delivery to regional lymph nodes, and upregulation of IL-6 mRNA expression by DNA hydrogel(CpG). (a) IL-6 release from DC2.4 cells. Cells were incubated with DNA samples at the indicated concentrations for 16 h. The IL-6 concentration in culture media was measured by ELISA, and was 1.7 ± 0.9 pg/ml in untreated DC2.4 cells. Results are expressed as the mean ± S.D. of three independent wells per sample. Data shown are representative of three independent experiments. All the data obtained with DNA hydrogel(CpG) were statistically significant compared with the other groups. (b, c) Time course of radioactivity in the injection site (b) and in draining lymph nodes (c) after intradermal injection of ^{32}P-DNA. Mice were injected with ^{32}P-ssDNA(CpG), ^{32}P-hexapodna(CpG) or ^{32}P-DNA hydrogel(CpG) at a DNA dose of 10 mg/kg (220 μg/mouse) into the dorsal skin. At the indicated times, the skin tissue including the injection site (b) and the draining lymph nodes (c) were collected, and radioactivity was counted. Data are normalized to the injected dose and are expressed as the mean ± S.D. of three mice. Data shown are representative of three independent experiments. (d, e) mRNA expression of IL-6 in the injection site (d) and in draining lymph nodes (e) after intradermal injection of DNA. Mice were injected with DNA samples at a dose of 220 μg/mouse into the dorsal skin. At the indicated times, the IL-6 mRNA expression was evaluated by real-time PCR. Results are normalized to the internal control β-actin gene, and are expressed as the mean ± S.D. of three or four mice. Data shown are representative of three independent experiments. *P < 0.05 compared with ssDNA(CpG) and all the GpC groups, #P < 0.05 compared with all the others at the same time point.

Tissue distribution of DNA hydrogel in mice. To trace the tissue distribution of DNA samples after injection into the dorsal skin of mice, ssDNA(CpG)$_{8np\text{-}32}$-A1 was end-labeled with ^{32}P using [γ-^{32}P]ATP and T4 polynucleotide kinase, and ^{32}P-labeled ssDNA(CpG), hexapodna(CpG), and DNA hydrogel(CpG) were prepared as described above. Figure 3b shows the time course of ^{32}P radioactivity in the dorsal skin of mice. After injection of ^{32}P-ssDNA(CpG) or ^{32}P-hexapodna(CpG), ^{32}P radioactivity quickly disappeared from the injection site. In stark contrast, ^{32}P radioactivity remained at the injection site for a longer period after injection of ^{32}P-DNA hydrogel(CpG) with a half-life of about 12 h. The injection of ^{32}P-DNA hydrogel(CpG) resulted in a slow and sustained accumulation of ^{32}P radioactivity in the lymph nodes (Figure 3c).

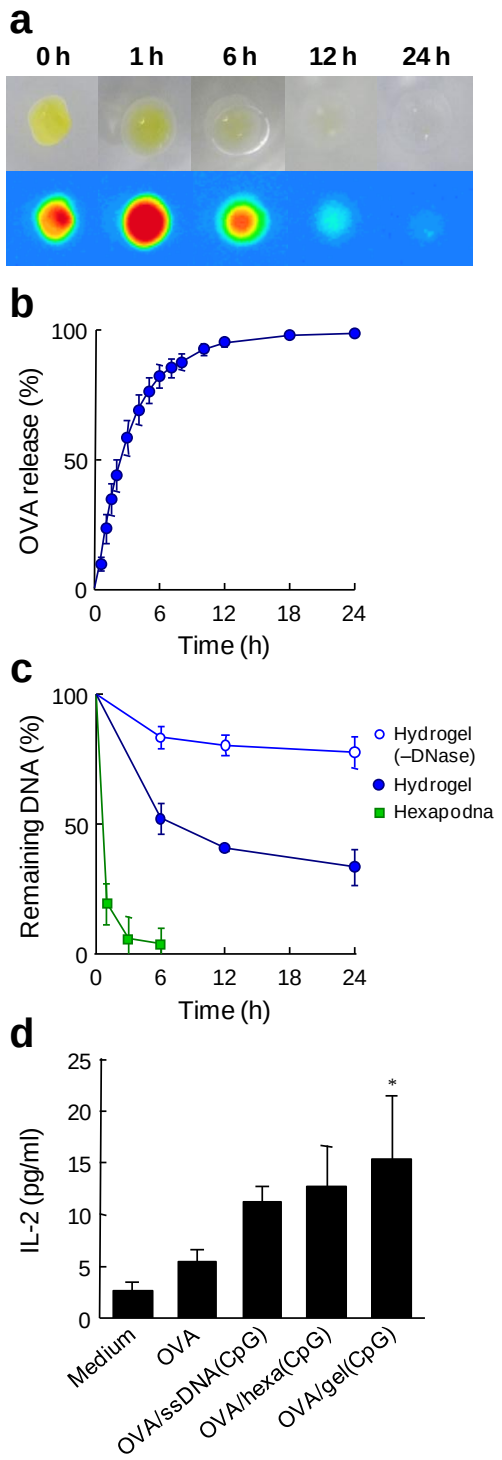

Correlation between tissue distribution of CpG DNA and elevated IL-6 expression. An injection of ssDNA(CpG) resulted in a slight increase in the mRNA expression (Figure 3d). On the other hand, an injection of hexapodna(CpG) or DNA hydrogel(CpG) significantly increased the IL-6 expression at the injection site 6 h after injection. The expression remained high for the experimental period of 24 h only in the DNA hydrogel(CpG) group. Similar profiles of IL-6 mRNA expression were observed in the draining lymph nodes (Figure 3e). There was no large increase in the IL-6 concentration in the serum after injection of DNA samples into the dorsal skin (Figure S2), indicating that DNA hydrogel(CpG) induces IL-6 expression at local sites where they accumulate.

Figure 4. OVA release from DNA hydrogel and antigen presentation in dendritic cells. (a, b) Time course of OVA release from DNA hydrogel. FITC-OVA (50 μg) was encapsulated into 220 μg of DNA hydrogel(CpG) and placed into the upper chamber of the Transwell (0.4 μm pore size) with the bottom chamber containing PBS, and incubated at 37 °C. The bright field (a, upper) and fluorescent images (a, lower) of the gel were photographed at the indicated times. The concentration of FITC-OVA in the bottom chamber was measured and plotted against time (b). Results are expressed as the mean ± S.D. of three wells per sample. Data shown are representative of three independent experiments. (c) Degradation of DNA hydrogel and hexapodna by DNase I. DNA samples were incubated at 37 °C in the presence of DNase I and the remaining amounts of DNA were plotted

against time. Results are expressed as mean ± S.D. of three independent determinations per sample. (d) IL-2 secretion from CD8OVA1.3 cells. DC2.4 cells (5×10^4 cells/well) were added with OVA (2 mg/ml) and CpG DNA (2 μg/ml), and incubated for 24 h. Thereafter, CD8OVA1.3 cells (5×10^4 cells/well) were added to each well and incubated for an additional 24 h. The IL-2 concentration in culture media was measured by ELISA. Results are expressed as the mean ± S.D. of three independent determinations per sample. Data shown are representative of two independent experiments. *$P < 0.05$ compared with the OVA alone group.

Sustained release of OVA from DNA hydrogel. In order to visualize OVA release, we first encapsulated fluorescein isothiocyanate (FITC)-labeled OVA, a model antigen, into DNA hydrogel(CpG) consisting of hexapodna$(CpG)_{8np\text{-}32}$-A and hexapodna$(CpG)_{8np\text{-}32}$-B. Figure 4a shows the bright-field and fluorescent images of FITC-OVA/DNA hydrogel(CpG). The hydrogel was swollen for the first 1 h, and a yellow color representing FITC-OVA was gradually diluted with time. The fluorescent images clearly show the slow release of FITC-OVA from DNA hydrogel(CpG). The fluorescence intensity measurement showed that FITC-OVA was gradually released from the DNA hydrogel (Figure 4b) with a half-life of 2.5 h (Figure S3). Figure 4c shows the degradation of DNA hydrogel(CpG) and hexapodna$(CpG)_{8np\text{-}32}$-A in buffer solution with or without DNase I. DNA hydrogel(CpG) was much more resistant to degradation than hexapodna$(CpG)_{8np\text{-}32}$-A.

Enhanced presentation of OVA by DNA hydrogel. DC2.4 mouse dendritic cells were incubated with OVA in the presence or absence of DNA, and then CD8OVA1.3 T hybridoma cells that recognize an OVA peptide ($OVA_{257–264}$) were added and incubated for additional 24 h. The addition of ssDNA(CpG), hexapodna(CpG) or DNA hydrogel(CpG) resulted in a significant increase in IL-2 production compared with the OVA group (Figure 4d).

Induction of anti-OVA immune response in mice. Mice were immunized with OVA with or without DNA by three intradermal injections at weekly intervals. Complete Freund's adjuvant (CFA), which is highly potent but severely toxic, was used as a positive control. DNA hydrogel(CpG) significantly increased the OVA specific total IgG titer in mouse serum compared with ssDNA(CpG) or hexapodna(CpG) groups (Figure 5a). Splenocytes of mice immunized with OVA/DNA hydrogel(CpG) produced significantly higher amounts of IFN-γ compared with those immunized with other formulations after restimulation with OVA (Figure 5b). The immunization with OVA/DNA hydrogel(CpG) induced significant cytotoxic T lymphocyte (CTL) responses against EG7-OVA cells, a cell line derived from the murine lymphoma EL-4 cells transfected with OVA cDNA (Figure 5c) but not against EL4 cells (Figure 5d). When OVA and DNA hydrogel(CpG) were administered separately to the dorsal skin (OVA) and to the footpad (DNA hydrogel), all the parameters examined were lower than those of the combined OVA/DNA hydrogel(CpG) group (Figure S4). OVA/DNA hydrogel(CpG) induced no significant changes at the injection site or in spleen weight, in contrast to OVA injected with CFA or alum, which is used in some vaccine formulations (Figure S5).

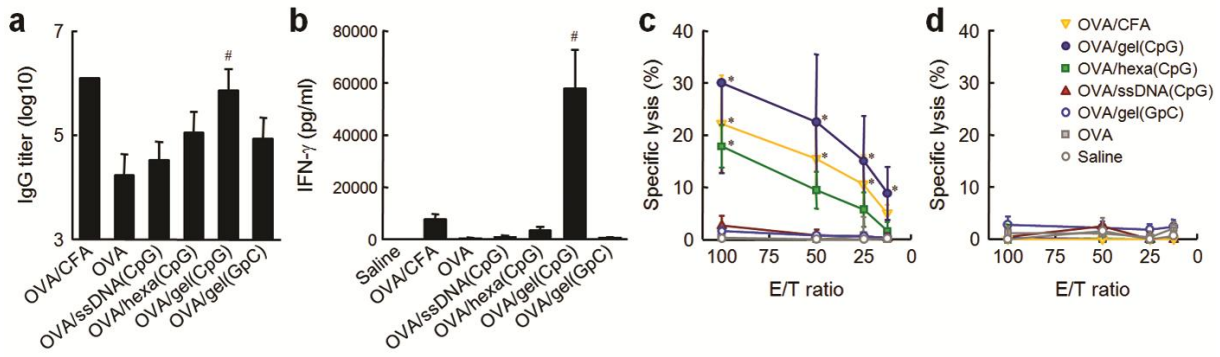

Figure 5. Induction of OVA specific immune responses after intradermal injection of OVA into mice. (a) OVA-specific total IgG in mouse serum after immunization. Mice were immunized with OVA with or without DNA by three intradermal injections at weekly intervals. At 7 days after the last immunization, the OVA-specific total IgG levels in serum were measured by ELISA. Serum total IgG titers were estimated by the dilution ratio at which the absorbance value of the saline group was obtained. Results are expressed as mean ± S.D. of three or four mice. Data shown are representative of three independent experiments. #$P < 0.05$ compared with all the other OVA/DNA groups. (b) IFN-γ production from splenocytes after re-stimulation with OVA. At seven days after the last immunization, splenocytes collected were added with OVA (1 mg/ml), and incubated for 4 days. The IFN-γ concentration in culture media was measured by ELISA. Results are expressed as mean ± S.D. of three or four mice. Data shown are representative of two independent experiments. #$P < 0.05$, statistically significant compared with the other groups. (c, d) CTL activity after immunization of mice with OVA. Seven days after the last immunization, splenocytes collected (5×10^7 cells) were co-cultured with mitomycin C-treated EG7-OVA (5×10^6 cells) for 5 days. EG7-OVA (c) or EL4 (d) were labeled with ^{51}Cr as target cells and co-incubated with the effector cells at the indicated ratio for 4 h. Results are expressed as mean ± S.D. of three or four mice. Data shown are representative of two independent experiments. *$P < 0.05$ compared with the OVA alone group.

DISCUSSION

Recent development of DNA nanotechnology has produced a large variety of DNA-based nano- and macrosystems [26-29]. One such system is DNA hydrogel, and several groups, including ours, have reported preparative methods and applications of DNA hydrogel systems [16-19]. The DNA-based material developed here was the hydrogel exhibiting the elasticity under small strain as shown in Figure 2a. In addition, the material did not flow with its own weight but was easily injected through a fine-gauged needle, which also indicates that the material is a gel. The DNA hydrogel developed in the present study has several unique and superior properties to other DNA hydrogels. First, it is injectable through an extra-fine, 29-gauge syringe. Injectable systems are much better than implantable ones when administered to patients. Second, no chemicals or synthetic compounds are needed for hydrogel preparation and gelation. Short DNA are the only components of the hydrogel, except for water and salts; this greatly enhances biocompatibility and biodegradability. Finally, hydrogel is an important system for sustained delivery of bioactive compounds [30-32]. Thus, the DNA hydrogel developed in this study provides a useful system for their sustained delivery. Some superior properties of the DNA hydrogel are attributed to the structural and thermal properties of nano-sized polypodna preparations that are designed and constructed using DNA nanotechnology. As demonstrated herein, DNA hydrogel can be developed either as an immunostimulatory system or in an immunologically inert mode.

The lower activity of hexapodna indicates that (1) DNA hydrogel is actually formed after injection, and (2) gel formation is important for the induction of OVA-specific immune

responses. Clearance of topically injected DNA is mediated mainly by DNase-mediated degradation and by absorption into systemic circulation [33]. Gel formation interferes with the degradation because of the reduced free terminals as well as of steric hindrance. The absorption of compounds from the injection site is a function of molecular size, so that gel formation is a requisite for the slow clearance of DNA samples. At that point, OVA or other incorporated molecules can then be slowly released from the hydrogel. Since Liu et al. demonstrated that assembled antigen-CpG DNA complexes were useful for inducing antigen-specific antibody responses [34], conjugates or complexes of OVA and CpG hexapodna may also be useful for the induction of OVA-specific immune responses. This possibility will be examined in future studies.

Crucially, we found that the DNA hydrogel undergoes very quick network reformation. Analysis of the modulus data suggested that the hydrogel is reorganized in a time scale of 0.25 s. This property is quite different from that of most hydrogel systems [24]. When the hydrogel is stressed, a fraction of the bonds is dissociated and, at the same time, the resulting free ends change partner and quickly reassociate through hydrogen bonds. This dissociation/association process allows the DNA hydrogel to be injected through an extra-fine needle and to return quickly to the gel state after injection.

The sharp difference between DNA hydrogel(CpG) and DNA hydrogel(GpC) clearly indicate that the recognition of CpG DNA by TLR9 is involved in the OVA-specific immune responses. Several studies using CpG DNA (which in most cases is phosphorothioate-modified) showed that the immunostimulation is important for antigen-specific immune responses [35-37]. The limited functions of ssDNA or hexapodna indicate that sustained OVA release is critical for induction of OVA-specific immune responses.

DNA hydrogel can be prepared from a wide variety of ODNs that can be custom-designed to fit the specific purpose. Thus, although our hydrogel described here was very effective, we cannot yet conclude that it is optimized for the induction of OVA-specific immune responses. This is since all the properties of DNA hydrogel, i.e., the immunostimulatory activity, the release rate of OVA, in vivo stability/degradation, are determined by its components. The optimization of these properties should be examined in future studies.

CONCLUSIONS

We have developed an injectable, self-gelling, biodegradable, and immunostimulatory DNA hydrogel using ODNs containing immunostimulatory CpG motifs, and proved that the hydrogel is an efficient system for sustained delivery of OVA, and for induction of the antigen-specific immune responses. Because the gel formation can be controlled by the salt concentration, the hydrogel can be delivered not only via injection but also packaged in spray or inhalation applications.

ACKNOWLEDGMENTS

This work was supported in part by a Grant-in-Aid for Scientific Research (B) (23390010) from Japan Society for the Promotion of Science (JSPS) and by a Grant-in-Aid for Scientific Research on Innovative Areas “Carcinogenic spiral” (25114706) from Ministry of Education, Culture, Sports, Science and Technology of Japan.

REFERENCES

[1] J.H. Chen, N.C. Seeman, Synthesis from DNA of a molecule with the connectivity of a cube, Nature 350 (1991) 631-633.

[2] P.W. Rothemund, Folding DNA to create nanoscale shapes and patterns, Nature 440 (2006) 297-302.

[3] Y. Li, Y.D. Tseng, S.Y. Kwon, L. D'Espaux, J.S. Bunch, P.L. McEuen, D. Luo, Controlled assembly of dendrimer-like DNA, Nat. Mater. 3 (2004) 38-42.

[4] S.H. Um, J.B. Lee, S.Y. Kwon, Y. Li, D. Luo, Dendrimer-like DNA-based fluorescence nanobarcodes, Nat. Protoc. 1 (2006) 995-1000.

[5] Y. He, T. Ye, M. Su, C. Zhang, A.E. Ribbe, W. Jiang, C. Mao, Hierarchical self-assembly of DNA into symmetric supramolecular polyhedra, Nature 452 (2008) 198-201.

[6] G. Hartmann, R.D. Weeratna, Z.K. Ballas, P. Payette, S. Blackwell, I. Suparto, W.L. Rasmussen, M. Waldschmidt, D. Sajuthi, R.H. Purcell, H.L. Davis, A.M. Krieg, Delineation of a CpG phosphorothioate oligodeoxynucleotide for activating primate immune responses in vitro and in vivo, J. Immunol. 164 (2000) 1617-1624.

[7] W. Barchet, V. Wimmenauer, M. Schlee, G. Hartmann, Accessing the therapeutic potential of immunostimulatory nucleic acids, Curr. Opin. Immunol. 20 (2008) 389-395.

[8] H. Hemmi, O. Takeuchi, T. Kawai, T. Kaisho, S. Sato, H. Sanjo, M. Matsumoto, K. Hoshino, H. Wagner, K. Takeda, S. Akira, A Toll-like receptor recognizes bacterial DNA, Nature 408 (2000) 740-745.

[9] M. Roman, E. Martin-Orozco, J.S. Goodman, M.D. Nguyen, Y. Sato, A. Ronaghy, R.S. Kornbluth, D.D. Richman, D.A. Carson, E. Raz, Immunostimulatory DNA sequences function as T helper-1-promoting adjuvants, Nat. Med. 3 (1997) 849-854.

[10] D.M. Klinman, Immunotherapeutic uses of CpG oligodeoxynucleotides, Nat. Rev. Immunol. 4 (2004) 249-258.

[11] A.M. Krieg, Therapeutic potential of Toll-like receptor 9 activation, Nat. Rev. Drug Discov. 5 (2006) 471-484.

[12] E.J. Hennessy, A.E. Parker, L.A. O'Neill, Targeting Toll-like receptors: emerging therapeutics? Nat. Rev. Drug Discov. 9 (2010) 293-307.

[13] J. Karbach, A. Neumann, C. Wahle, K. Brand, S. Gnjatic, E. Jäger, Therapeutic administration of a synthetic CpG oligodeoxynucleotide triggers formation of anti-CpG antibodies, Cancer Res. 72 (2012) 4304-4310.

[14] M. Nishikawa, M. Matono, S. Rattanakiat, N. Matsuoka, Y. Takakura, Enhanced Immunostimulatory activity of oligodeoxynucleotides by Y-shape formation, Immunology 124 (2008) 247-255.

[15] K. Mohri, M. Nishikawa, N. Takahashi, T. Shiomi, N. Matsuoka, K. Ogawa, M. Endo, K. Hidaka, H. Sugiyama, Y. Takahashi, Y. Takakura, Design and development of nanosized DNA assemblies in polypod-like structures as efficient vehicles for immunostimulatory CpG motifs to immune cells, ACS Nano 6 (2012) 5931-5940.

[16] S.H. Um, J.B. Lee, N. Park, S.Y. Kwon, C.C. Umbach, D. Luo, Enzyme-catalysed assembly of DNA hydrogel, Nat. Mater. 5 (2006) 797-801.

[17] M. Nishikawa, Y. Mizuno, K. Mohri, N. Matsuoka, S. Rattanakiat, Y. Takahashi, H. Funabashi, D. Luo, Y. Takakura, Biodegradable CpG DNA hydrogels for sustained delivery of doxorubicin and immunostimulatory signals in tumor-bearing mice, Biomaterials 32 (2011) 488-494.

[18] E. Cheng, Y. Xing, P. Chen, Y. Yang, Y. Sun, D. Zhou, L. Xu, Q. Fan, D. Liu, A pH-triggered, fast-responding DNA hydrogel, Angew. Chem. Int. Ed. Engl. 48 (2009) 7660-7663.
[19] Y. Xing, E. Cheng, Y. Yang, P. Chen, T. Zhang, Y. Sun, Z. Yang, D. Liu, Self-assembled DNA hydrogels with designable thermal and enzymatic responsiveness, Adv. Mater. 23 (2011) 1117-1121.
[20] M. Nishikawa, T. Otsuki, A. Ota, X. Guan, S. Takemoto, Y. Takahashi, Y. Takakura, Induction of tumor-specific immune response by gene transfer of Hsp70-cell-penetrating peptide fusion protein to tumors in mice, Mol. Ther. 18 (2010) 421-428.
[21] J.D. Ferry, Viscoelastic Properties of Polymers, 3rd ed., Wiley, New York, 1980.
[22] N. Kobayashi, T. Kuramoto, K. Yamaoka, M. Hashida, Y. Takakura, Hepatic uptake and gene expression mechanisms following intravenous administration of plasmid DNA by conventional and hydrodynamics-based procedures, J. Pharmacol. Exp. Ther. 297 (2001) 853-860.
[23] X. Guan, M. Nishikawa, S. Takemoto, Y. Ohno, T. Yata, Y. Takakura, Injection site-dependent induction of immune response by DNA vaccine: comparison of skin and spleen as a target for vaccination, J. Gene Med. 12 (2010) 301-309.
[24] R. Larson, The Structure and Rheology of Complex Fluids; Oxford University Press, New York, 1999.
[25] S. Rattanakiat, M. Nishikawa, H. Funabashi, D. Luo, Y. Takakura, The assembly of a short linear natural cytosine-phosphate-guanine DNA into dendritic structures and its effect on immunostimulatory activity, Biomaterials 30 (2009) 5701-5706.
[26] N.C. Seeman, An overview of structural DNA nanotechnology, Mol. Biotechnol. 37 (2007) 246-257.
[27] M. Nishikawa, S. Rattanakiat, Y. Takakura, DNA-based nano-sized systems for pharmaceutical and biomedical applications, Adv. Drug Deliv. Rev. 62 (2010) 626-632.
[28] A.V. Pinheiro, D. Han, W.M. Shih, H. Yan, Challenges and opportunities for structural DNA nanotechnology, Nat. Nanotechnol. 6 (2011) 763-772.
[29] J.B. Lee, S. Peng, D. Yang, Y.H. Roh, H. Funabashi, N. Park, E.J. Rice, L. Chen, R. Long, M. Wu, D. Luo, A mechanical metamaterial made from a DNA hydrogel, Nat. Nanotechnol. 7 (2012) 816-820.
[30] A.S. Hoffman, Hydrogels for biomedical applications, Adv. Drug Deliv. Rev. 54 (2002) 3-12.
[31] S. Young, M. Wong, Y. Tabata, A.G. Mikos, Gelatin as a delivery vehicle for the controlled release of bioactive molecules, J. Control. Release 109 (2005) 256-274.
[32] T. Nochi, Y. Yuki, H. Takahashi, S. Sawada, M. Mejima, T. Kohda, N. Harada, I.G. Kong, A. Sato, N. Kataoka, D. Tokuhara, S. Kurokawa, Y. Takahashi, H. Tsukada, S. Kozaki, K. Akiyoshi, H. Kiyono, Nanogel antigenic protein-delivery system for adjuvant-free intranasal vaccines, Nat. Mater. 9 (2010) 572-578.
[33] P.A. Cossum, L. Truong, S.R. Owens, P.M. Markham, J.P. Shea, S.T. Crooke, Pharmacokinetics of a ^{14}C-labeled phosphorothioate oligonucleotide, ISIS 2105, after intradermal administration to rats, J. Pharmacol. Exp. Ther. 269 (1994) 89-94.
[34] X. Liu, Y. Xu, T. Yu, C. Clifford, Y. Liu, H. Yan, Y. Chang Y, A DNA nanostructure platform for directed assembly of synthetic vaccines, Nano Lett. 12 (2012) 4254-4259.

[35] A.K. Yi, J.G. Yoon, A.M. Krieg, Convergence of CpG DNA- and BCR-mediated signals at the c-Jun N-terminal kinase and NF-κB activation pathways: regulation by mitogen-activated protein kinases, Int. Immunol. 15 (2003) 577-591.
[36] D.M. Klinman, D. Currie, I. Gursel, D. Verthelyi, Use of CpG oligodeoxynucleotides as immune adjuvants, Immunol. Rev. 199 (2004) 201-216.
[37] D. Valmori, N.E. Souleimanian, V. Tosello, N. Bhardwaj, S. Adams, D. O'Neill, A. Pavlick, J.B. Escalon, C.M. Cruz, A. Angiulli, F. Angiulli, G. Mears, S.M. Vogel, L. Pan, A.A. Jungbluth, E.W. Hoffmann, R. Venhaus, G. Ritter, L.J. Old, M. Ayyoub, Vaccination with NY-ESO-1 protein and CpG in montanide induces integrated antibody/Th1 responses and CD8 T cells through cross-priming, Proc. Natl. Acad. Sci. USA 104 (2007) 8947-8952.

FIGURE LEGENDS

Figure 1. Formation of DNA hydrogel without DNA ligase. (a) Hydrogel formation after drop wise addition of tetrapodna preparations into a buffer solution. Tetrapodna preparations were labeled using PI. Far left, tetrapodna$(CpG)_{12p\text{-}28}$-A in a buffer solution containing 5 mM sodium chloride. Second from the left, a solution containing the physiological sodium chloride concentration of 154 mM. Third from the left, tetrapodna$(CpG)_{12p\text{-}28}$-A added to the solution containing physiological sodium chloride concentration. Far right, tetrapodna$(CpG)_{12np\text{-}28}$-A added to the solution containing physiological sodium chloride concentration. (b) An FE-SEM image of the inner structure of DNA hydrogel consisting of tetrapodna$(CpG)_{12p\text{-}28}$-A. (c, d) Hydrogel formation in syringe and injection through a 29-gauge needle. Hexapodna$(GpC)_{8np\text{-}32}$-A and hexapodna$(GpC)_{8np\text{-}32}$-B (right, DNA hydrogel[GpC]) or hexapodna$(GpC)_{8np\text{-}32}$-A and hexapodna$(GpC)_{8np\text{-}32}$-C (left), all of which were labeled using PI, were mixed in a 29-gauge insulin syringe (c), then injected (d). (e, f) Hydrogel formation in mouse skin after intradermal injection. Hexapodna$(GpC)_{8np\text{-}32}$-A and hexapodna$(GpC)_{8np\text{-}32}$-B (e, DNA hydrogel(GpC)) or hexapodna$(GpC)_{8np\text{-}32}$-A and hexapodna$(GpC)_{8np\text{-}32}$-C (f) was injected into the dorsal skin of mice at a dose of 30 mg/kg (660 μg/mouse), and the skin was collected and observed at 3 h after injection.

Figure 2. Rheological characterization of DNA hydrogel exhibiting quick reorganization of hydrogen bonds at room temperature (~25 °C). (a) and (b) Storage and loss moduli (G' and G'') measured for sinusoidal strain at various angular frequencies ω and with the amplitude γ_0 as indicated. In panels (a) and (b), respectively, the G' and G'' data are plotted against ω in the double-logarithmic scale. The dotted curves in panel (b) indicate the G' data for amplitude γ_0 = 0.005 and 0.1 (0.5 % and 10 %). The minimum of G' at $\omega = 4\ s^{-1}$ observed for large γ_0 is indicative of the network reorganization process at a characteristic time $\tau \cong 0.25$ s. (c) Time evolution of the shear stress $\sigma^+(t)$ measured after start-up of shear flow at constant rates κ as indicated. The $\sigma^+(t)$ are plotted against the strain, $\gamma = \kappa t$. (d) Steady state shear stress σ_{ss} evaluated from the $\sigma^+(t)$ data shown in Fig. 2c. The σ_{ss} data are plotted against the shear rate κ and the dynamic yield stress, $\sigma_{y,dyn} \cong 13$ Pa, is evaluated from those data at low κ. Data shown are representative of two independent experiments.

Figure 3. IL-6 production, sustained delivery to regional lymph nodes, and upregulation of IL-6 mRNA expression by DNA hydrogel(CpG). (a) IL-6 release from DC2.4 cells. Cells were incubated with DNA samples at the indicated concentrations for 16 h. The IL-6 concentration in culture media was measured by ELISA, and was 1.7 ± 0.9 pg/ml in untreated DC2.4 cells. Results are expressed as the mean ± S.D. of three independent wells per sample. Data shown are representative of three independent experiments. All the data obtained with DNA hydrogel(CpG) were statistically significant compared with the other groups. (b, c) Time course of radioactivity in the injection site (b) and in draining lymph nodes (c) after intradermal injection of ^{32}P-DNA. Mice were injected with ^{32}P-ssDNA(CpG), ^{32}P-hexapodna(CpG) or ^{32}P-DNA hydrogel(CpG) at a DNA dose of 10 mg/kg (220 μg/mouse) into the dorsal skin. At the indicated times, the skin tissue including the injection site (b) and the draining lymph nodes (c) were collected, and radioactivity was counted. Data are normalized to the injected dose and are expressed as the mean ± S.D. of three mice. Data shown are representative of three independent experiments. (d, e) mRNA expression of IL-6 in the injection site (d) and in draining lymph nodes (e) after intradermal injection of DNA. Mice were injected with DNA samples at a dose of 220 μg/mouse

into the dorsal skin. At the indicated times, the IL-6 mRNA expression was evaluated by real-time PCR. Results are normalized to the internal control β-actin gene, and are expressed as the mean ± S.D. of three or four mice. Data shown are representative of three independent experiments. *P < 0.05 compared with ssDNA(CpG) and all the GpC groups, #P < 0.05 compared with all the others at the same time point.

Figure 4. OVA release from DNA hydrogel and antigen presentation in dendritic cells. (a, b) Time course of OVA release from DNA hydrogel. FITC-OVA (50 μg) was encapsulated into 220 μg of DNA hydrogel(CpG) and placed into the upper chamber of the Transwell (0.4 μm pore size) with the bottom chamber containing PBS, and incubated at 37 °C. The bright field (a, upper) and fluorescent images (a, lower) of the gel were photographed at the indicated times. The concentration of FITC-OVA in the bottom chamber was measured and plotted against time (b). Results are expressed as the mean ± S.D. of three wells per sample. Data shown are representative of three independent experiments. (c) Degradation of DNA hydrogel and hexapodna by DNase I. DNA samples were incubated at 37 °C in the presence of DNase I and the remaining amounts of DNA were plotted against time. Results are expressed as mean ± S.D. of three independent determinations per sample. (d) IL-2 secretion from CD8OVA1.3 cells. DC2.4 cells (5×10^4 cells/well) were added with OVA (2 mg/ml) and CpG DNA (2 μg/ml), and incubated for 24 h. Thereafter, CD8OVA1.3 cells (5×10^4 cells/well) were added to each well and incubated for an additional 24 h. The IL-2 concentration in culture media was measured by ELISA. Results are expressed as the mean ± S.D. of three independent determinations per sample. Data shown are representative of two independent experiments. *P < 0.05 compared with the OVA alone group.

Figure 5. Induction of OVA specific immune responses after intradermal injection of OVA into mice. (a) OVA-specific total IgG in mouse serum after immunization. Mice were immunized with OVA with or without DNA by three intradermal injections at weekly intervals. At 7 days after the last immunization, the OVA-specific total IgG levels in serum were measured by ELISA. Serum total IgG titers were estimated by the dilution ratio at which the absorbance value of the saline group was obtained. Results are expressed as mean ± S.D. of three or four mice. Data shown are representative of three independent experiments. #P < 0.05 compared with all the other OVA/DNA groups. (b) IFN-γ production from splenocytes after re-stimulation with OVA. At seven days after the last immunization, splenocytes collected were added with OVA (1 mg/ml), and incubated for 4 days. The IFN-γ concentration in culture media was measured by ELISA. Results are expressed as mean ± S.D. of three or four mice. Data shown are representative of two independent experiments. #P < 0.05, statistically significant compared with the other groups. (c, d) CTL activity after immunization of mice with OVA. Seven days after the last immunization, splenocytes collected (5×10^7 cells) were co-cultured with mitomycin C-treated EG7-OVA (5×10^6 cells) for 5 days. EG7-OVA (c) or EL4 (d) were labeled with ^{51}Cr as target cells and co-incubated with the effector cells at the indicated ratio for 4 h. Results are expressed as mean ± S.D. of three or four mice. Data shown are representative of two independent experiments. *P < 0.05 compared with the OVA alone group.